RSC Publishing Journal of Materials Chemistry B

Tailoring hierarchical meso-macroporous 3D scaffolds: From nano to macro

Journal:	*Journal of Materials Chemistry B*
Manuscript ID:	TB-ART-09-2013-021307.R1
Article Type:	Paper
Date Submitted by the Author:	18-Oct-2013

Complete List of Authors:	Cicuéndez, Mónica; Complutense University Of Madrid, Inorganic and Bioinorganic Chemistry Malmsten, Martin; Uppsala University, Department of Pharmacy Doadrio, Juan; Complutense University Of Madrid, Inorganic and Bioinorganic Chemistry Portoles, Teresa; Complutense University Of Madrid, Biochemistry and Molecular Biology I Izquierdo-Barba, Isabel; Complutense University Of Madrid, Inorganic and Bioinorganic Chemistry Vallet-Regi, Maria; Universidad Complutense de Madrid, Spain,

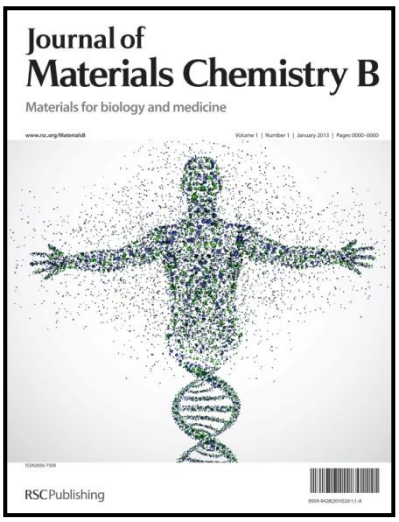

Journal of Materials Chemistry B

Materials for Biology and Medicine

Full paper submission

Journal of Materials Chemistry B is a weekly journal in the materials field. The journal is interdisciplinary, publishing work of international significance on all aspects of materials chemistry related to biology and medicine. Articles cover the fabrication, properties and applications of materials.

2012 Impact Factor of *Journal of Materials Chemistry*: **6.10**
For more information go to www.rsc.org/materialsB

The following paper has been submitted to *Journal of Materials Chemistry B* for consideration as a **full paper**.

Journal of Materials Chemistry B wishes to publish original research that demonstrates **novelty and advance**, either in the chemistry used to produce materials or in the properties/applications of the materials produced. Work submitted that is outside of these criteria will not usually be considered for publication. The materials should also be related to the theme of materials for biology and medicine.

Routine or incremental work, however competently researched and reported, should not be recommended for publication if it does not meet our expectations with regard to novelty and impact.

It is the responsibility of authors to provide fully convincing evidence for the homogeneity and identity of all compounds they claim as new. Evidence of both purity and identity is required to establish that the properties and constants reported are those of the compound with the new structure claimed.

Thank you for your effort in reviewing this submission. It is only through the continued service of referees that we can maintain both the high quality of the publication and the rapid response times to authors. We would greatly appreciate if you could review this paper in **two weeks**. Please let us know if that will not be possible.

Once again, we appreciate your time in serving as a reviewer. To acknowledge this, the RSC offers a **25% discount** on its books: http://www.rsc.org/Shop/books/discounts.asp. Please also consider submitting your next manuscript to *Journal of Materials Chemistry B*.

Best wishes,

Liz Dunn
Managing Editor, *Journal of Materials Chemistry B*

Mónica Cicuéndez[a,b], Martin Malmsten[c], Juan Carlos Doadrio[a], María Teresa Portolés[d], Isabel Izquierdo-Barba[a,b*] and María Vallet-Regía,[b*]

J. Mater. Chem. B. xxxx, **xx**, xxxx

Tailoring hierarchical meso-macroporous 3D scaffolds from nano to macro

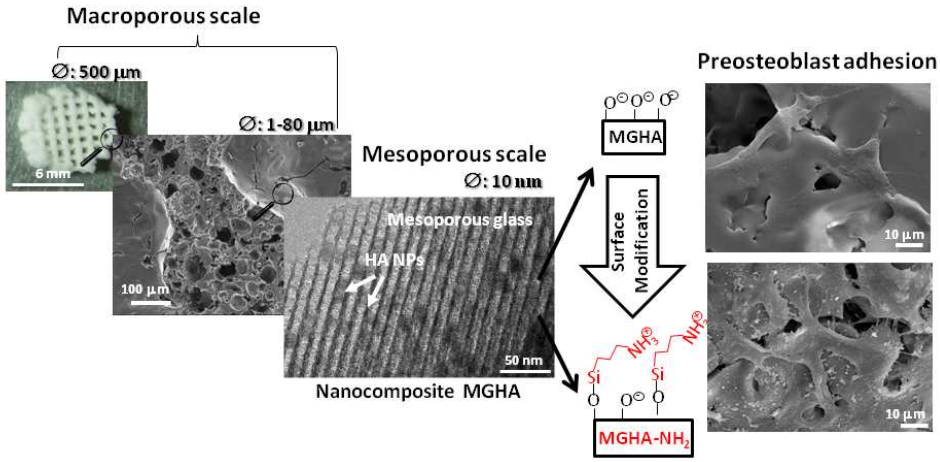

Hierarchical 3D scaffolds based on new hydroxyapatite/mesoporous glass nanocomposite bioceramic (MGHA) exhibiting different scales of porosity have been synthesized have been obtain by rapid prototyping process. Moreover, to improve the surface properties of these scaffolds concerning cell recognition, direct functionalization with aminopropyl moieties was carried out. This simple and cost-effective amine modification notably provokes improvements in the preosteoblast adhesion, proliferation (2.3 folds), differentiation (4.8 folds), and further scaffold colonization. These results suggest that both the structure design and the amine chemical modification of their surface significantly improve the potential of these nanocomposite materials for bone tissue regeneration purposes.

Journal of Materials Chemistry B RSCPublishing

ARTICLE

Tailoring hierarchical meso-macroporous 3D scaffolds: From nano to macro

Cite this: DOI: 10.1039/xoxxoooooox

Mónica Cicuéndez[a,b], Martin Malmsten[c], Juan Carlos Doadrio[a], María Teresa Portolés[d], Isabel Izquierdo-Barba[a,b]* and María Vallet-Regí[a,b]*

Received ooth January 2012,
Accepted ooth January 2012

DOI: 10.1039/xoxxoooooox

www.rsc.org/

Bone tissue regeneration requires the use of 3D scaffolds which mimic the architecture of the natural extracellular matrix, creating an adequate microenvironment for bone cell growth. Such 3D scaffolds need surface properties suitable to biological recognition in the early stage of cell adhesion, necessary to assure complete cell colonization, retained cell functionality, and subsequently bone regeneration. Herein, hierarchical 3D scaffolds based on new hydroxyapatite/mesoporous glass nanocomposite bioceramic (MGHA) exhibiting different scales of porosity have been synthesized. These possess: (i) highly ordered mesopores with diameters of 10 nm; (ii) macropores with diameters in the 30–80 μm range with interconnections of 1-10 μm; and (iii) large macropores of ca. 500 μm. To improve their surface properties, 3D scaffolds were modified through direct functionalization with amine propyl groups, which notably improves preosteoblast adhesion, proliferation (2.3 fold), differentiation (4.8 fold) and further cell colonization of these scaffolds. The observed enhancement can be related to these amine groups which favour early adhesion, e.g., based on nonspecific protein adsorption as was demonstrated by ellipsometry. These results suggest that the combination of hierarchical structure design and amine surface modification of hydroxypatite/mesoporous nanocomposite scaffolds, yields a double increase in cell proliferation, as well as quadruple increase in cell differentiation, demonstrating the potential of these nanocomposite materials for bone tissue regeneration purposes.

1. Introduction

Bone tissue engineering requires the use of tridimensional (3D) scaffolds which act as temporary templates for migration, proliferation, and differentiation of cells to guide bone repair, stimulating natural mechanisms of bone regeneration.[1-3] These processes are affected by both pore structure at different length scales and the chemical surface composition of these implants, which constitute fundamental pillars in the design and manufacture of these scaffolds.[1] The scaffold macroporous architecture should maintain the mechanical integrity of the material during bio-resorption, but also sustain both cell proliferation and new extracellular matrix deposition. *In vivo* studies have shown that interconnected macropores in the range of 150-500 μm and porosity over 50% led directly to bone mineralization.[4-6] Moreover, pore interconnection is directly related to vascularisation and nutrient diffusion, both critical for osteogenesis.[5] Furthermore, it has been established that the nanoscale in the scaffold surface has important implication in the control of cell behaviour. In fact, natural bone has nanoscale dimensions, where the extracellular matrix (ECM) is mainly constituted by collagen-fiber framework (10-300 nm) with interconnected nanopores, and hydroxyapatite nanocrystals (25-4 nm).[7,8] Thus, several studies have shown that nanostructured porous surfaces significantly enhance cell attachment, cell viability, alkaline phosphatase (ALP) activity, and gene expression of osteoblasts on hydroxyapatite scaffolds.[9]

However, most synthetic 3D scaffolds lack chemical surface properties involved in the biological recognition processes and in the early stage of cell adhesion, necessary to assure the complete cell colonization for subsequently bone regeneration.[6,10] Cell adhesion is the first event in the recognition between the 3D scaffold surface and cells, playing a primary role in posterior cellular responses.[11,12] This process depends on both non-specific and specific cell/biomaterial surface interactions with cooperative effects.[11] Non-specific cell adhesion through physical/chemical interactions is responsible of the early stage of cell adhesion, which involves the contact of the biomaterial surface with the pericellular coat (PCC) containing hyaluronan, highly negatively charged under the physiological condition.[13,14] Subsequently, specific adhesion mechanisms are triggered by conjugation of extracellular ligands to receptors in the cell membrane.[12] These receptors are heterodimeric transmembrane proteins called integrins, which, in a natural environment, interact with adhesion peptide sequences of extracellular matrix proteins.[15]

Numerous studies have been focused on the anchoring of specific adhesion peptides, e.g., RGD, peptide to enhance both processes.[1,16-18] These approaches are, however, expensive and

require high control of peptide location and final conformation on the scaffold surface. In fact, cell adhesion on these modified supports is often not significantly better than on commercialized tissue-culture plastic (TCP), based on a simple functionalization with lysine moieties on the plate surface.[19] In this sense, TCP exhibits good cell adhesion due to their capability to enable absorption of proteins in culture medium and then enhances non-specific adhesion of cells. Based on this strategy, there is a considerable interest in using simple chemistry to improve cell responses, addressing the incorporation of positively charged amino moieties in the biomaterial surface which significantly favour cell adhesion and further differentiation.[20,21]

Recently, a nanocomposite bioceramic (MGHA), formed by particles of nanocrystalline apatite embedded into amorphous mesoporous bioactive glass in the SiO_2-P_2O_5-CaO system, has been reported.[22] Due to the synergy of the features of its two components, including (i) ordered mesoporous arrangement with pores of 8 nm, (ii) high surface area and pore volume, (iii) high bioactivity, (iv) presence of nanocrystalline apatite particles homogeneously distributed, and (v) improved *in vitro* biocompatibility, this nanocomposite material is an excellent candidate for bone tissue engineering. However, with this objective, it is necessary to obtain 3D macroporous scaffolds based on this nanostructured material with the porosity ranges required for proper cell colonization, preserving the intrinsic characteristics of both components during the scaffolds manufacturing process. The aim of the present study was therefore to prepare hierarchical meso-macroporous MGHA 3D scaffolds in one-pot process by the combination of different meso- and macro-structural directing agents through the rapid prototyping (RP) technique. Moreover, to improve the cell adhesion and the scaffold colonization, a simple surface functionalization with aminopropyl groups directly on the scaffolds was also carried out. MC3T3 preosteoblast proliferation and differentiation on these MGHA 3D scaffolds were analysed to confirm the performance of the scaffold design, while ellipsometry was employed for investigating the potential role of protein adsorption for cell adhesion.

2. Materials and Methods

2.1. MGHA 3D scaffolds preparation

3D scaffolds based on mesoporous glass/hydroxyapatite nanocomposite (MGHA) were prepared by rapid prototyping (RP) via direct-write assembly of precursor slurry using an EnvisionTEC GmbH Prefactory® 3D Bioplotter™ (Gladbeck, Germany). This RP technique constitutes an excellent alternative for manufacture of scaffolds suitable for different clinical applications and individuals.[23] The slurry is derived of a sol precursor of MGHA nanocomposite previously synthesized in powder,[22] to which was added methylcellulose (MC) to produce a slurry with a suitable consistency to be extruded during the RP process.[24,25] In a typical synthesis, 19.5 g of F127 was dissolved in 168.6 mL of absolute ethanol (99.5%, Panreac) with 12.8 mL of 1.0 M HCl (prepared from 37% HCl, Panreac) solution and 19.4 mL of Milli-Q water. Afterwards, the appropriate amounts of tetraethyl orthosilicate (TEOS, 98%, Sigma−Aldrich), triethyl phosphate (TEP, 99.8%, Sigma−Aldrich), and calcium chloride ($CaCl_2$•$4H_2O$, 99%, Sigma−Aldrich) as SiO_2, P_2O_5, and CaO sources, respectively, were added in 1h intervals under continuous stirring during 4 h at 40°C and subsequently maintained in static conditions at the same temperature overnight. Subsequently, the MGHA sol precursor was aged 4-5 days until reaching a final volume reduction of ≈ 30% through evaporation-induced self-assembly (EISA). Then, MC was added under vigorous stirring in a F127/MC molar ratio of 6 obtaining a suitable consistency to be extruded in the RP process. Cylindrical 50x133x38 mm scaffolds were designed and fabricated layer-by-layer by direct ink deposition over a plate at room temperature. Each layer was pre-designed showing a 90° rotation with respect to the previous. To obtain the best results, the dispensing speed and pressure were slightly modified from the initial machine parameters during the dispensing process for each scaffold. The scaffold hardening process occurred by solvent evaporation and the pieces were left to dry at 30ºC. Finally, the pieces were calcined at 700º C for 6 h.

2.2. Amine functionalization of MGHA 3D scaffolds

Nanocomposite MGHA 3D scaffolds were functionalized directly post-synthesis with amine groups using 3-aminopropyltriethoxysilane ($C_9H_{23}NO_3Si$, APTES, ≥ 98% wt, Sigma-Aldrich). In doing so, two scaffold pieces (25 mg of weight per piece) were degassed overnight at 100ºC, followed by addition of 12.5 mL of dried toluene (98%, Aldrich). Subsequently, 0.5 mL of APTES reactant was incorporated and kept 12 h in reflux under a nitrogen atmosphere at 80ºC. Then, the scaffolds were removed and washed in aqueous medium in continuous stirring during 24h. The resulting amine functionalized scaffolds are denoted MGHA-NH_2.

2.3. Characterization

X-ray diffraction (XRD) experiments were performed on a Philips X'Pert diffractometer (Eindhoven, The Netherlands), equipped with Cu Kα (40 kV, 20 mA). Transmission electron microscopy (TEM) was performed on a JEOL 3010 electron microscope (Jeol Ltd., Japan), operating at 300 kV (Cs; 0.6 mm, resolution 1.7 °A). All TEM images were recorded employing a CCD camera (MultiScan model 794, Gatan Inc., UK) under low-dose conditions. Fourier transform (FT) patterns were extracted from the images of thin crystal regions using a Digital Micrograph (Gatan Inc., UK). Scanning electron microscopy (SEM) was performed using a field emission JEOL JSM-6335F microscope (Tokyo, Japan) at an acceleration voltage of 10 kV. Textural properties were determined by N_2 adsorption porosimetry using a Micromeritics ASAP2020 analyzer (Norcross, USA). Prior to these measurements, both MGHA and MGHA-NH_2 scaffolds were degassed at 60ºC during 24 hours under vacuum (<0.3 kPa). The surface area was determined using the multipoint Brunauer–Emmett–Teller method included in the software. The porosity of 3D scaffolds was measured by mercury intrusion porosimetry in a Micromeritics Autopore IV 9500 device (Micromeritics Instrument Corporation, Norcross, GA, USA). Elemental analyses (C, H, N) were carried out on a LECO CHNS-932 microanalyzer (Saint Joseph, Michigan USA). Fourier transform Infrared (FTIR) spectroscopy was performed in a Thermo Nicolet Nexus spectrometer (Thermo Scientific, USA) from 4000 to 400 cm^{-1}, using the KBr pellet method and operating in transmittance mode. ^{29}Si, ^{31}P and ^{13}C single pulse (SP) and cross-polarization (CP)/MAS (magic angle spinning) solid-state nuclear magnetic resonance (NMR) measurements were performed to evaluate the different silicon, phosphorus, and carbon environments in synthesized scaffolds. NMR spectra were recorded on a Bruker Avance 400 WB

spectrometer (Karlsruhe, Germany). Samples were spun at 10, 6, and 12 kHz for ^{29}Si, ^{31}P and ^{13}C, respectively. These spinning speeds were sufficient to make the spinning sidebands of low intensity and outside the region of interest. Spectrometer frequencies were set to 79.49, 161.97, and 75.45 MHz for ^{29}Si, ^{31}P, and ^{13}C, respectively. Chemical shift values were referenced to 3-trimethylsilyl-1-propanesulfonic acid sodium salt (DDS), 85% phosphoric acid (H_3PO_4) and glycine for ^{29}Si, ^{31}P, and ^{13}C, respectively. Time periods between successive accumulations were 5, 4, and 3 ms for ^{29}Si, ^{31}P, and ^{13}C, respectively, and the number of scans was ca. 13,000 for all spectra. Zeta-potential (ζ) measurements were performed on a Malvern Zetasizer Nano Series instrument (Malvern Instruments Ltd., UK). For this purpose, 10 mg of each powdered sample was added to 20 mL of KCl solution (20mM) and the mixture vigorously stirred to reach a homogenous suspension. The measurements were carried out at in pH range of 2-10 by addition of HCl solution (0.01M) and NaOH (0.01M). Six ζ-potential runs were recorded for each sample at 37 ºC, with a minimum of 30 sub runs per measure, where after average values and standard deviations were calculated (n = 6).

2.4. Protein adsorption

Hydrophilic and negatively charged silica surfaces were prepared from polished silicon slides (p-type, boron doped). The surfaces were cleaned in a mixture of 25% NH_4OH, 30% H_2O_2, and H_2O (1:1:5, by volume) at 80°C for 5 min, followed by cleaning in a mixture of 32% HCl, 30% H_2O_2, and H_2O (1:1:5, by volume) at 80°C for 5 min. The slides were then rinsed twice with water and ethanol. This procedure rendered the surfaces hydrophilic, with a water-air contact angle of less than 10°. MGHA was deposited on these silica slides through dip-coating method using the MGHA precursor sol aged for 24 hours at room temperature, with a withdrawal rate of 2,500 mm/s. The coatings were dried at 100ºC (1 h) and annealed in air at 700 ºC for 1 hour to remove the surfactant and to produce the MGHA nanocomposite phase. Finally, the coatings were washed with ethanol in an ultrasonic bath for 2 min. Homogeneous MGHA coatings were obtained confirmed by SEM and EDS studies. Subsequently, these coatings were amine functionalized by the same procedure, this time using APTES moieties as functionalizing agent. The effectiveness of amine functionalization process was confirmed by FTIR and XRD analyses. Fibrinogen adsorption to such MGHA deposited on silica surfaces was studied *in situ* by null ellipsometry, using an Optrel Multiskop (Optrel, Kleinmachnow, Germany) equipped with a 100 mW argon laser. All measurements were carried out at 532 nm and an angle of incidence of 67.66° in a 5 ml cuvette under stirring (300 rpm). Both the principles of null ellipsometry and the procedures used have been described extensively before.[26] In brief, by monitoring the change in the state of polarization of light reflected at a surface in the absence and presence of an adsorbed layer, the mean refractive index (n) and layer thickness (d) of the adsorbed layer can be obtained. From the thickness and refractive index the adsorbed amount (Γ) was calculated according to:

$$\Gamma = \frac{(n - n_0)}{dn/dc} d$$

where n_0 is the refractive index of the bulk solution, and dn/dc the refractive index increment (0.154 cm^3/g). Corrections were routinely done for changes in bulk refractive index caused by changes in temperature and excess electrolyte concentration.

2.5. Cell adhesion, morphology, mitochondrial activity and cell differentiation

2.5.1. Cell culture

MGHA and MGHA-NH_2 scaffolds were sterilized under UV light for 15 min and then submerged in Dulbecco´s Modified Eagle´s Medium (DMEM, Sigma Chemical Company, St. Louis, MO, USA) supplemented with penicillin (800 µg/mL, BioWhittaker Europe, Belgium), streptomycin (800 µg/mL, BioWhittaker Europe, Belgium), β-glycerolphosphate (50 µg/mL, Sigma Chemical Company, St. Louis, MO, USA) and L- ascorbic acid (10 mM, Sigma Chemical Company, St. Louis, MO, USA), under a CO_2 (5%) atmosphere at 37ºC for 24 h to stabilize before cell culture. Subsequently, murine MC3T3-E1 preosteoblasts (as undifferentiated osteoblast-like cells) were seeded at a density of 10^5 cells/mL in DMEM with 10% fetal bovine serum (FBS, Gibco, BRL), 1 mM L-glutamine (BioWhittaker Europe, Belgium), penicillin (200 µg/mL, BioWhittaker Europe, Belgium), and streptomycin (200 µg/mL, BioWhittaker Europe, Belgium), under a CO_2 (5%) atmosphere at 37ºC for 48 h.

2.5.2. Morphological studies by Scanning Electron Microscopy

For SEM studies, cells attached to the 3D scaffolds were fixed with glutaraldehyde (2.5% in Phosphate Buffer Saline, PBS) for 45 min. Sample dehydration was performed by slow water replacement, using a series of ethanol solutions (30%, 50%, 70%, 90%) for 30 min with a final dehydration in absolute ethanol for 60 min, allowing samples to dry at room temperature and under vacuum. Afterwards, the pieces were mounted on stubs and coated in vacuum with gold-palladium. Cells were examined with a JEOL JSM-6400 scanning electron microscope.

2.5.3. Mitochondrial activity

To evaluate cell mitochondrial activity of living cells on MGHA and MGHA-NH_2 3D scaffolds, as well as around them (in the bottoms of the cell culture wells) after 48 h of incubation, an MTT method was employed, based in the reduction of yellow 3[4,5-dimethylthiazol-2yl]-2,5-diphenyltetrazolium bromide to blue formazan.[27] For this, the culture media were replaced with 1 mL of DMEM and 125 µL of 0.012 g/L MTT solution in PBS. Samples were incubated for 4 h at 37ºC and 5% CO_2 in dark conditions. Then, the medium was removed and 500 µL of isopropanol:HCl 0.4 N were added. Finally, the absorbance was measured at 570 nm using a Helios Zeta UV-VIS spectrophotometer.

2.5.4. Alkaline phosphatase activity

Alkaline phosphatase (ALP) activity of cells growing on the both MGHA and MGHA-NH_2 scaffolds was used as the key differentiation marker in assessing expression of the osteoblast phenotype. ALP activity was measured using the Reddi and Huggins method based on the hydrolysis of p-nitrophenylphosphate to p-nitrophenol [28]. For this, MC3T3 cells (5 x 10^4 cells/mL) were seeded directly onto scaffolds in 24-well plates and incubated under standard culture conditions

using supplemented medium with β-glycerolphosphate (50 μg/mL, Sigma Chemical Company, St. Louis, MO, USA) and L- ascorbic acid (10 mM, Sigma Chemical Company, St. Louis, MO, USA). In order to evaluate ALP activity both in and around the scaffolds after 7 days incubation, each scaffold was transferred to a new well. Moreover, the protein total value after 7 days was determined by a colorimetric method at 540 nm (Bio-Analítica, S.L.), using a Helios Zeta UV-VIS spectrophotometer.

2.6. Statistics

Data are expressed as means ± standard deviations of three experiments. Statistical analysis was performed using the Statistical Package for the Social Sciences (SPSS) version 11.5 software. Statistical comparisons were made by analysis of variance (ANOVA). Scheffé test was used for *post hoc* evaluations of differences among groups. In all statistical evaluations, $p < 0.05$ was considered as statistically significant.

3. Results and discussion

3.1 MGHA 3D scaffolds and cell colonization

The macroporosity of the MGHA 3D scaffolds obtained by RP technique was characterized by SEM and Hg intrusion porosimetry. Digital photograph (inset Fig. 1A) displays the image of a cylindrical piece of MGHA scaffold. SEM micrograph (Fig. 1A) shows that MGHA scaffolds consist of a lattice of rods stacked with simple tetragonal symmetry according to the RP computer-aided design, where twenty layers of mesh were stacked to a total thickness of *ca*. 2 mm, with a diameter of ≈ 6.6 mm. These scaffolds present a hierarchical pore network with macropores around 500 μm connected by rods of 250-300 μm diameter, corresponding to the porosity required for tissue growth and vascularization in the human body.[29,30] Higher magnification SEM micrograph, corresponding to a scaffold cross-section (Fig. 1B), shows notable differences between the interior and exterior scaffold surface. While the external surface exhibits cylinders with relatively smooth topography and a small fraction of pores in the range between 1-10 μm, the interior surface exhibits numerous pores in the range of 30 to 80 μm, resulting from the MC calcination process.[24,25] Moreover, Hg intrusion porosimetry shows that the internal larger pores are accessible to the liquid probe, indicating well connected macroporous systems (data not shown). Total percentage porosity is of 60%, mainly in the 1-10 μm and 100-300 μm range according to SEM images. Low angle XRD patterns of these scaffolds (Fig. 1C) show three diffraction maxima at 0.86, 1.43, and 1.67° (2θ), which can be indexed as (10), (11), and (20) reflections of a 2D hexagonal structure (*P6mm* plane group) based on TEM results (Fig. 1D). N_2 isotherms (Table 1) demonstrate the presence of a very narrow distribution of large mesopores centred at 10 nm, with a surface area and pore volume of 123 m^2/g and 0.2 cm^3/g, respectively. Compared to the powder MGHA nanocomposite, the results obtained for the MGHA 3D scaffolds reveal a notable increase in pore size, from 8.0 nm for powder nanocomposite[22] to 10 nm for scaffold, accompanied by a decrease both in surface area and pore volume. This increase in pore size can be attributed to MC incorporation during the synthesis process.[31]

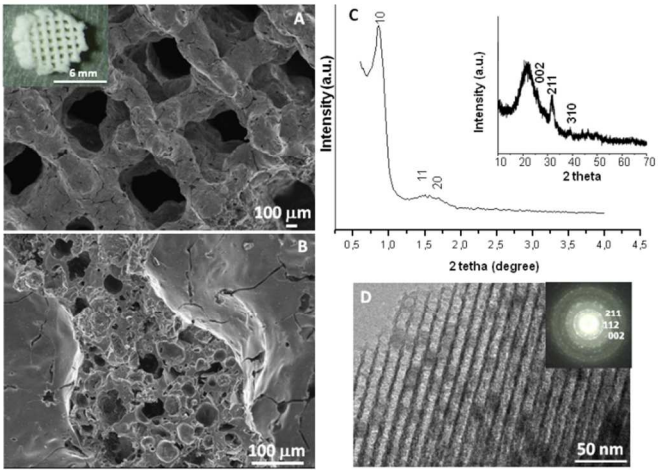

Fig. 1 Macro- and mesostructural characterization of hierarchical interconnected MGHA nanocomposite 3D scaffold. Surface (A) and cross-transversal section (B) obtained by SEM. (Inset) Digital photograph of a MGHA scaffold. (C) XRD pattern at low scattering angles showing the ordered mesoporous arrangement. (Inset) XRD pattern at wide scattering angles demonstrates the presence of apatite phase. (D) TEM image showing the homogeneous distribution of the nanocrystalline apatite particles into the 2D hexagonal mesoporous structure. (Inset) ED pattern.

Table 1 Textural parameters corresponding to MGHA scaffolds before and after amine functionalization. Amount of aminopropyl moieties covalently bound to the scaffolds was determined by CHN elemental analyses and ζ-potential at pH physiological.

Sample	S_{BET} (m^2/g)	V_p (cm^3/g)	D_p (nm)	mmol APTES	ζ mV
Powder MGHA*	235	0.4	8.0	-	-25 ±5
MGHA scaffold	123	0.2	10.0	-	-35±6
MGHA-NH_2scaffold	101	0.2	8.6	1.55	+8±3

** corresponds to powder MGHA nanocomposite previously reported in the reference.*[22]

To confirm the presence of nanocrystalline apatite in the MGHA 3D scaffolds, XRD and TEM studies were carried out. Wide-angle XRD patterns (Inset, Fig. 1C) show very broad (002), (211) and (310) reflections, which could be attributed to apatite occurrence.[32] Furthermore, TEM studies (Fig. 1D) showed small darker zone homogeneously distributed into the mesoporous structure corresponding to a nanocrystalline apatite phase particles. Electron diffraction (inset) of a dark zone displayed diffuse halos, showing d-spacing at 0.28, 0.27, and 0.34 nm, corresponding to apatite phase. Thus confirms the nanocomposite structure of scaffolds, indicating that the incorporation of the MC polymer in the synthesis for the scaffolding process did not affect the biphasic structure of MGHA.

Therefore, the single-step sol–gel route synthesis in presence of a surfactant (F127) as mesostructure directing agent and a biomacromolecular polymer (methylcellulose) as macrostructure template, followed by RP technique, allows the formation of the hierarchical interconnected 3D scaffolds exhibiting different scales of porosity: (i) highly ordered mesopores with diameters of *ca.*10 nm that may act as local controlled delivery systems of biologically active molecules, and allow better supply nutrient diffusion;[33-35] (ii) interconnected macropores with diameters in the 1–80 μm, and (iii) ultra-large macropores of *ca.* 500 μm, that may provide the

opportunities for cell colonization.[29] Furthermore, the presence of nanocrystalline apatite particles homogeneously distributed along the composite constitutes one more common element with the bone structure and may influence and control protein interactions through its surface properties, guiding cellular responses as it occurs in the natural bone.[36] Thus, this combination of the macroporous architecture, the nanoscale structure of the surface, and presence of apatite particles may provide real benefits for MGHA nanocomposite scaffolds in bone tissue regeneration.

To investigate whether the MGHA scaffold architecture and composition would permit good bone integration, cell morphology, spreading degree, and internalization of MC3T3 preosteoblasts were studied after 2 days culture at different levels (depth) inside the macroporous structure. L1 label indicates the outer level, while L2 and L3 correspond to inner macropores, respectively. Fig. 2A shows low magnification SEM micrograph evidencing the presence of cells anchored through filopodia projections (inset) on the surface of L1, L2, and L3 zones, demonstrating that the MGHA scaffolds are colonized over the entire visible surface. Fig. 2B, 2C, and 2D provide details of the three levels in which cells exhibit a typical morphology for this cell type.[37]

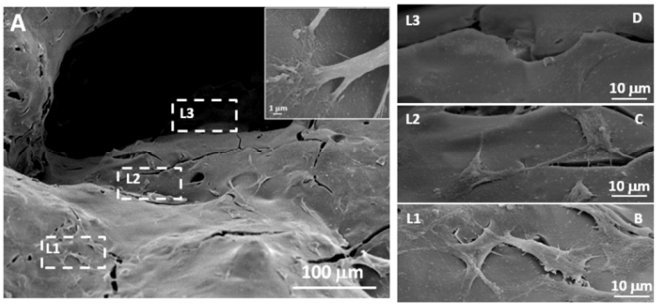

Fig. 2 SEM studies of MGHA 3D scaffold colonization by MC3T3 preosteoblasts A) Low magnification micrograph of cell adhesion and colonization at different macroporous levels (L1, L2, and L3) of the scaffold. (Inset) cell anchoring in detail. B), C), and D) Higher magnifications micrographs showing the details of spreading MC3T3 cells at these macroporous levels. All micrographs are representative from the study.

The obtained results revealed adequate cell colonization over the MGHA scaffold surface. A commonly used approach for making the scaffold surface more conductive to cell adhesion is its preconditioning with cell adhesive peptides or proteins.[16,17] In the present study, without any such preconditioning, the chemical and structural characteristics of these MGHA scaffolds are proved to be excellent in terms of biocompatibility. However, the cell number at the inner levels of these scaffolds could be improved by a proper surface treatment to enhance cell colonization.

3.2. Amine functionalization of 3D scaffold surface and its influence on cell adhesion, mitochondrial activity and cell differentiation

Since it has been demonstrated that surface chemistry of a material exerts an important influence on cell response,[7] amine functionalization of the 3D MGHA scaffolds surface was carried out. Fig. 3 displays FTIR spectra before and after amine functionalization, both spectra exhibiting bands corresponding to the MGHA nanocomposite material. Thus, the bands of Si-O bonds at 1040, 800, and 470 cm^{-1} correspond to the amorphous silica mesoporous glass, while the doublet at 560 and 600 cm^{-1} is characteristic of crystalline phosphate.[38] After amine functionalization, FTIR spectrum of the MGHA-NH_2 scaffold shows the appearance of new bands at 3344 and ca. 1500 cm^{-1}, corresponding to NH stretching and deformation frequencies, respectively, whereas bands at 3030 and ≈1590 $cm^{-1}$are attributed to $–NH_3^+$ stretching and deformation frequencies, respectively.[39,40] Moreover, the band at 2980 cm^{-1} corresponds to $–CH_2–$ groups, the band at 1260 cm^{-1} to the Si–C bond, and the small band at 1300 cm^{-1} to the C–N bond, confirm also the presence of organosilane (APTES).[40]

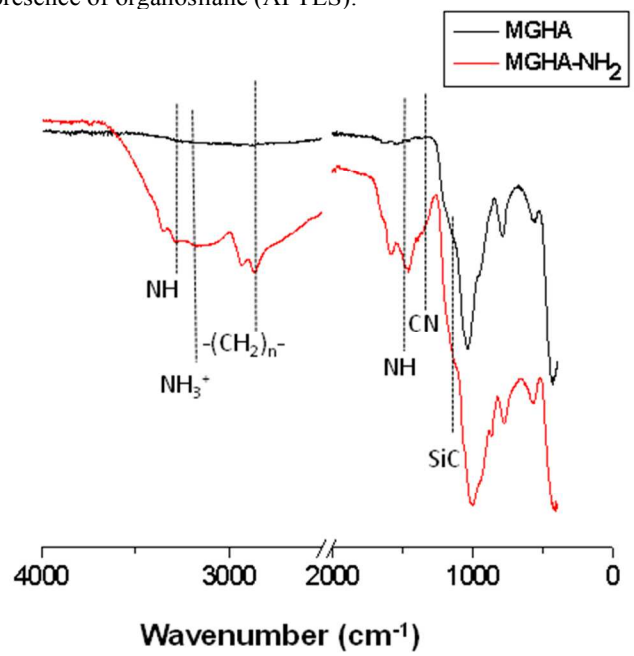

Fig. 3 FTIR spectra corresponding to MGHA 3D scaffold before and after amine functionalization.

To quantify the number of amine present on the surface of MGHA-NH_2 scaffold, a CHNS elemental chemical analysis was carried out. The experimental data indicated 0.02 mmol of APTES per square meter surface. Textural properties after functionalization process revealed a slight decrease in the surface area, and pore diameter values (Table 1), indicating the incorporation of amino propyl silane moieties, maintaining the pore volume. Moreover, concerning meso-macroporosity, XRD, TEM, SEM, and Hg intrusion studies demonstrated that the both meso-macrostructural parameters were not altered after functionalization (data not shown).

^{29}Si and ^{31}P solid state SP and CP/MAS NMR measurements were carried out to further investigate the grafting of aminopropyl moieties to the MGHA scaffold surface as well as their condensation degree. Fig. 4 displays ^{29}Si MAS NMR spectra recorded from MGHA and MGHA-NH_2 3D scaffolds using single-pulse excitation, together with their component lines obtained from spectral deconvolutions. Both spectra show resonances at ca. -102 and -112 ppm, corresponding to $Q^3[Si(OSi)^3(OX)]$, and $Q^4[Si(OSi)_4]$ silicon sites, respectively (X=H, C). No significant changes are observed in Q^3/Q^4 relative populations after functionalization process. The presence of signals attributable to T^n units [$R\text{-}Si(OSi)_n\text{-}(OX)_{3-n}$] (X = H,C) are indicative of the organosilane groups, only evidenced in the MGHA-NH_2 3D scaffold. The presence of T^3 and T^2 signals demonstrates the existence of covalent linkages between the silica surface and the organic

groups.[41] Table 2 confirms that no significant changes occur in the $Q^2/Q^3/Q^4$ and $q^2/q^1/q^0$ relative populations for ^{29}Si and ^{31}P environments after functionalization process.

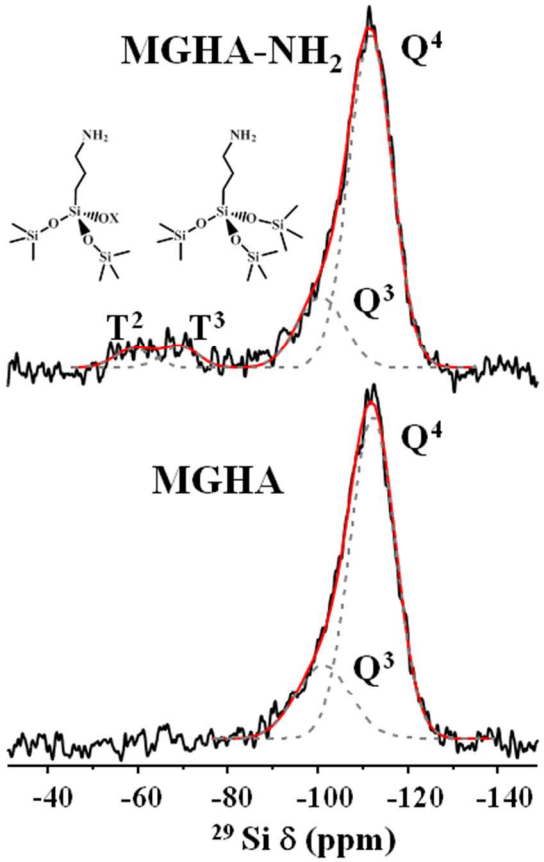

Fig. 4 Solid-state ^{29}Si single-pulse MAS NMR spectra (with their Q_n and T_n silicon environments) corresponding to 3D MGHA scaffold before and after amine functionalization. The areas for the Q_n and T_n units were calculated by Gaussian line-shape deconvolutions.

Table 2 Population percent of ^{29}Si and ^{31}P environments resulting of deconvoluting the experimental NMR spectra recorded by cross-polarization (CP) corresponding to unmodified and functionalized scaffolds. ([a] This NMR signal may comprise minor contributions from Q^2_{Ca} tetrahedral.[22])

Sample	^{29} Si CP					^{31} P CP		
	T^2 (%)	T^3 (%)	Q_H^2 (%)[a]	Q_H^3 (%)	Q^4 (%)	q^0 (%)	q^1 (%)	q^2 (%)
MGHA	-	-	19.7	57.2	23.1	65.7	32.2	2.1
MGHA-NH_2	45	55	16.8	46.8	36.4	55.5	35.7	8.8

Solid state ^{13}C CP/MAS NMR spectra were collected to confirm the surface functionalization of MGHA scaffolds and to get information concerning the ionization state of amine (Table 3). As expected, no signals are observed in the ^{13}C NMR spectrum of unmodified MGHA scaffold (data not shown). In contrast, after amine functionalization displays well defined signals at 11, 24, and 45 ppm, which can be assigned to carbon atoms from APTES in three different environments (Table 3). Note that there is no resonance at ca. 28 and 85 ppm which would be attributed to the central carbon of 3-aminopropyl chain of APTES with the $–NH_2$ group as nonprotonated form. The resonance appearing in the region of stronger fields, at 24 ppm, assignable to central carbon of APTES, evidences the protonation of 3-aminopropyl groups, as it has been also confirmed by FTIR data.[42,43]

Table 3 Data of solid state ^{13}C CP/MAS NMR corresponding to MGHA-NH_2 3D scaffold.

MGHA-NH_2	
δ (ppm)	**Assignment**
11	Si-**C**$\mathbf{H_2}$- CH_2-CH_2-NH_2
24	Si-CH_2-**C**$\mathbf{H_2}$- CH_2-NH_3^+
45	Si-CH_2- CH_2-**C**$\mathbf{H_2}$-NH_2

With the chemical nature of scaffolds clarified, their charge in aqueous media was investigated by ζ-potential measurements. Fig. 5A displays the ζ-potential of MGHA and MGHA-NH_2 scaffolds as a function of pH, and reveals notable differences before and after amine functionalization. Thus, at physiological pH 7.4, the ζ-potential was ≈-35 mV for unmodified MGHA scaffold. This negative surface charge is due to the presence of deprotonated species, i.e., $Si\text{-}O^-$ (pKa = 4.5) from mesoporous glass and $P–O^-$ species (pKa = 6.5) from apatite clusters. For MGHA-NH_2 scaffolds, on the other hand, the ζ–potential at pH 7.4 was +8 mV due to presence of NH_3^+species (pKa = 10.0). To confirm the pKa values corresponding to all functional groups present in the scaffold MGHA-NH_2, a titration curve was carried out between pH values from 10 to 4. Fig. 5B demonstrates that, in agreement with expected bibliographic data, pKa (NH_3^+) is 10.0; pKa (POH) is 6.3, and pKa (SiOH) is 4.5. These results demonstrate that at physiological pH (7.4), the majority species present in the surface scaffold could correspond to NH_3^+, PO^-, and SiO^- moieties.

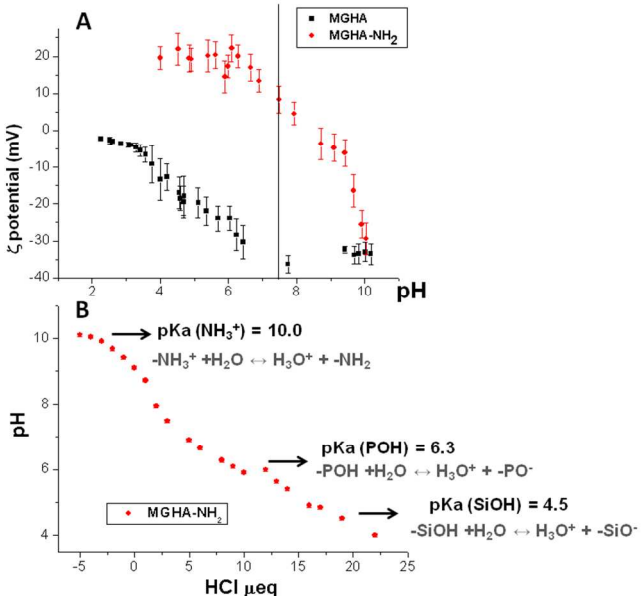

Fig. 5 (A) ζ potential curves as function of pH before and after amine functionalisation of MGHA nanocomposite 3D scaffolds. (B) Titration curve with HCl corresponding to MGHA-NH_2.

When cell adhesion on MGHA-NH_2 scaffolds was analyzed by SEM after 2 days culture, a multilayer of MC3T3 cells anchored through filopodia projections (inset Fig. 6) was observed throughout the surface of these scaffolds (Fig. 6A).

Compared to MGHA scaffolds (Fig. 2), a larger number of cells are observed colonizing all studied levels (L1, L2, and L3; Fig. 6B, 6C and 6D, respectively) of MGHA-NH_2 scaffold. In all cases there is multilayer cell growth, also at the inner level (L3). This multilayer growth at all levels demostrates intercellular communication which constitutes a fundamental pillar for total scaffold colonization, ensuring new bone in-growth.[44]

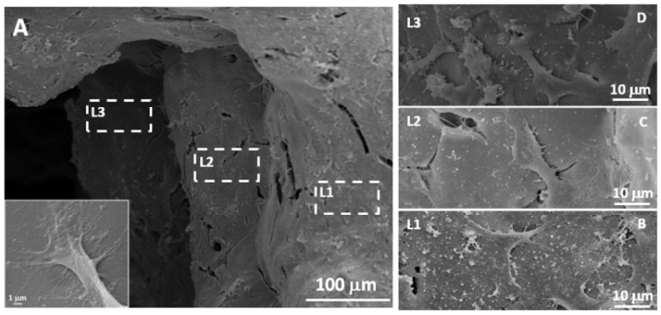

Fig. 6 A) SEM studies of MGHA-NH_2 scaffold colonization by MC3T3 preosteoblasts showing internalization and cell spreading of preosteoblast MC3T3 cells cultured for 2 days on amine functionalized 3D-MGHA scaffold at different macropore levels (L1, L2, and L3). Inset: Detail of the filopodia projections. B), C) and D) Higher magnification SEM micrographs of spreading MC3T3 cells in the different macropore levels. All micrographs are representative from the study.

This notable enhancement of cell colonization on MGHA-NH_2 with respect to unmodified MGHA scaffolds could be explained by the different surface chemistry of these samples. At physiological pH (7.4), the MGHA scaffold surface is negatively charged (-35 mV) due to the presence of SiO^- and PO^- groups, whereas after amine functionalization (MGHA-NH_2), the scaffold surface attains a positive surface charge (+8 mV) because of the presence of NH_3^+ groups. Thus, there is an increased direct electrostatic attractive interaction between cationic surfaces and negatively charged membrane cells.[45] In addition, the positive charge promotes adsorption of culture medium proteins, which are involved in the non-specific early stage of cell adhesion.[18] To confirm the role of the surface amine groups on protein adsorption, ellipsometry studies with both surfaces, MGHA and MGHA-NH_2, were carried out. In analogy to the increased cell adhesion, the amine functionalized surfaces display increased adsorption of serum proteins, exemplified for fibrinogen in Fig. 7. As can be seen, adsorption of this important serum protein is much higher for the cationic MGHA-NH_2 compared to unmodified and negatively charged MGHA. This is a reflection of the net negative charge of fibrinogen at these conditions (IEP≈5.5),[46] promoting its adsorption to the oppositely charged MGHA-NH_2 surface. This is in agreement with similar findings obtained for surfaces rendered cationic also by other approaches.[47] Particularly, for serum proteins stimulating cell adhesion, such as fibrinogen and fibronectin, the mechanism for promoting increased cell adhesion and spreading of the MGHA-NH_2 scaffold is likely facilitated by the formation of a conditioning protein layer.

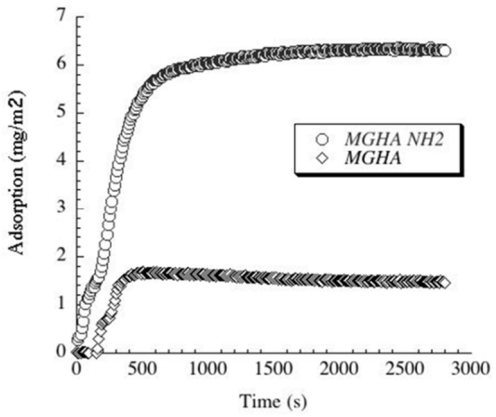

Fig. 7 Fibrinogen adsorption to MGHA and MGHA-NH_2 surfaces detected by ellipsometry.

Moreover, in order to investigate the broader potential of these 3D scaffolds, other cell parameters as mitochondrial activity and cell differentiation were evaluated. The results show a significant increase of mitochondrial activity (2.3 folds, $p \leq 0.05$) when the scaffold surface is previously amine functionalized (Fig. 8A) which is due to the higher number of cells on these scaffolds. Concerning MC3T3 preosteoblast differentiation, evaluated after 7 days culture by ALP activity per total protein, the results reveal a significant increase (4.8 folds, $p < 0.05$) of this cell differentiation parameter on MGHA-NH_2 scaffolds with respect to MGHA scaffolds and TCP control (Fig. 8B). Non-significant differences between MGHA scaffold and TCP control were observed ($p > 0.05$).

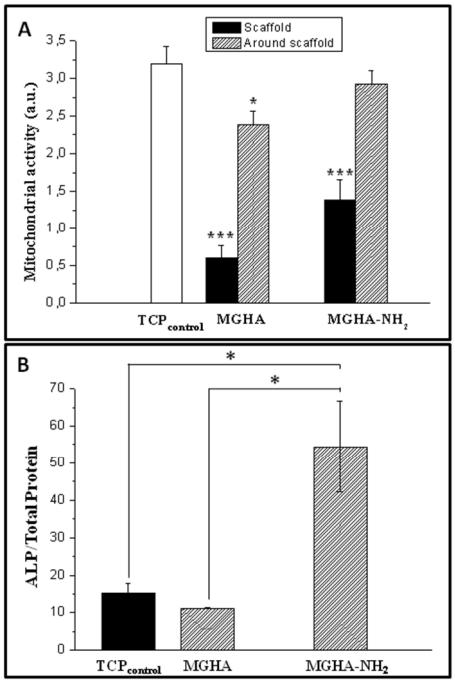

Fig. 8 A) Mitochondrial activity of preosteoblast MC3T3 cells on the surface scaffold and around scaffold of unmodified and amine modified ones after 2 days of incubation. B) ALP per total protein of preosteoblast MC3T3 cells on the surface scaffold of unmodified (MGHA) and amine modified (MGHA-NH_2) ones after 7 days of incubation. Statistical significance: *$p < 0.05$, ***$p < 0.005$.

Taken together, these results thus demonstrate that both the structure design of 3D MGHA scaffold at different length scales (macro and nanoscale) and the use of basic chemistry to incorporate simple amine functional groups to their surface enhance notably the cell adhesion, scaffold colonization and preosteoblast differentiation (Fig. 9).

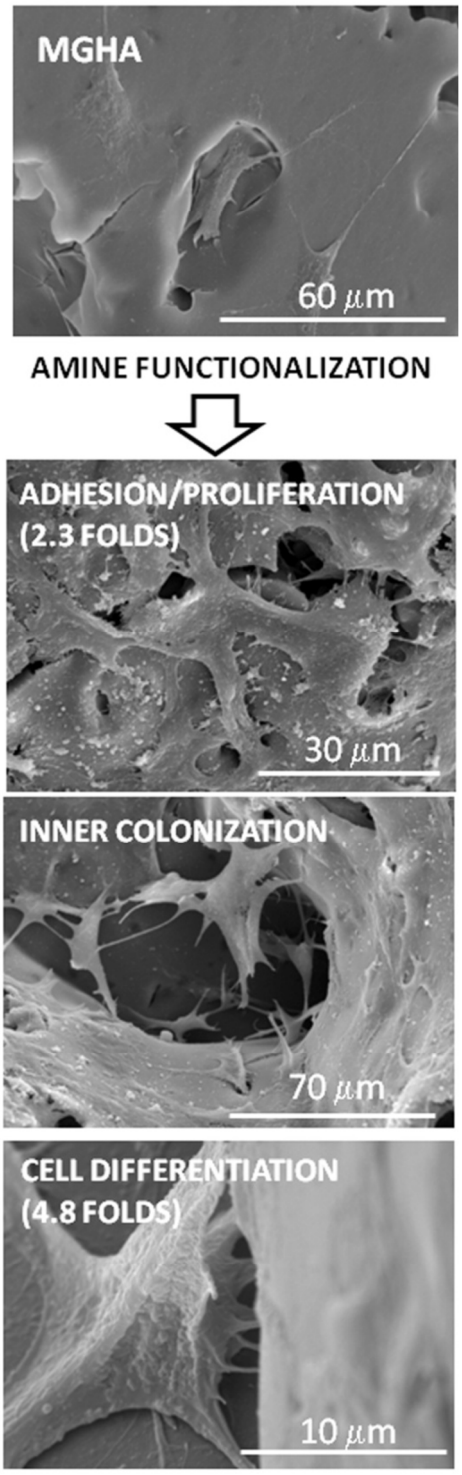

Fig. 9 Summary of effects produced by amine functionalisation of MGHA nanocomposite 3D scaffolds.

Conclusions

3D scaffolds based in a new nanocomposite (MGHA) composed by hydroxyapatite nanocrystalline embedded into mesoporous glass have been fabricated through rapid prototyping technique. The 3D MGHA scaffolds exhibit three scales of porosity: ordered mesopores (10nm), interconnected macropores (1-80μm), and ultra-large macropores (500μm). This hierarchical meso-macroporous system is obtained by using a sol precursor containing different scale-length polymers (Pluronic F127 and methylcellulose as meso and macrostructure directing agents, respectively) together with a robocasting process. The surface properties of these MGHA scaffolds, concerning cell recognition have been enhanced through a direct functionalization with aminopropyl moieties. This simple and cost-effective amine modification causes noticeable improvements in the preosteoblast adhesion, as well as a double increase in cell proliferation and a quadruple increase in cell differentiation. Moreover, ellipsometry studies demonstrated that the protonated amino propyl moieties favour the early step in the adhesion process by an increase in the nonspecific protein adsorption. Therefore, these studies reveal that both the structure design of hierarchical meso-macroporous 3D MGHA scaffolds and the amine chemical modification of their surface significantly improve the biocompatibility of these nanocomposite scaffolds.

Acknowledgements

This study was supported by research grants from Comunidad de Madrid (S2009/MAT-1472) and Ministerio de Ciencia e Innovacion (MICINN) through the projects MAT2012-35556 and CS2010-11384-E. M. Cicuéndez is grateful to MICINN for the financial support through FPI fellowship. The authors wish to thank also to the staff of the ICTS Centro Nacional de Microscopia Electrónica (Spain) and Centro de Citometría y Microscopia de Fluorescencia, Centro de Difracción de Rayos X, Centro de Microanálisis Elemental and Centro de Resonancia Magnética Nuclear of the Universidad Complutense de Madrid (Spain).

Notes and references

[a] Departamento de Química Inorgánica y Bioinorgánica. Facultad de Farmacia. Universidad Complutense de Madrid. Plaza Ramón y Cajal s/n. 28040 Madrid. Spain.

[b] Networking Research Center on Bioengineering, Biomaterials and Nanomedicine (CIBER-BBN), Madrid, Spain.

[c] Department of Pharmacy, Uppsala University, SE-75123 Uppsala, Sweden.

[d] Departamento de Bioquímica and Biología Molecular I, Facultad de Ciencias Químicas, Universidad Complutense de Madrid, Ciudad Universitaria s/n, 28040-Madrid, Spain.

* Corresponding author: E-mail address: vallet@ucm.es, ibarba@ucm.es

1 S.J. Hollister. *Adv. Mater.* 2009, **21**, 330–3342.

2 R. Langer, J.P. Vacanti JP. *Science* 1993, **260**, 920–926.

3 T.G. Kim, H. Sim, D.W.Lin. *Adv Funct Mater* 2012, **22**, 2446–68.

4 X. Yu. Z. Xia, L. Wang. F. Peng, X. Jiang, J. Huang, D. Rowed, and M. Wei, *J. Mater. Chem.* 2012, 22, 9721–9730.
5 V. Karageorgiou, D. Kaplan. *Biomaterials* 2005, **26**, 5474–5491.
6 M. Vallet-Regí. *Chem. Eur. J.* 2006, **12**, 5934–5943.
7 M.M. Stevens, J.H.George. *Science* 2005, **310**, 1135–1138.
8 M. Vallet-Regi, J.M. Gonzalez-Calbet. *Progg. Solid State Chem.* 2004, **32**, 1–31.
9 L. Xia, K. Lin, X. Jiang, Y. Xu, M. Zhang, J. Chang, Z. Zhang. *J. Mater. Chem. B* DOI:10.1039/c3tb2094.
10 M. Vallet-Regí, M. Colilla, I. Izquierdo-Barba, *J. Biomed. Nanotech* 2008, **4**, 1–15
11 K. Anselme. *Biomaterials* 2000, **21**, 667–681.
12 B. Geiger, J.P. Spatz, A.D. Bershadsky. *Nat. Rev. Mol. Cell Biol.* 2009, **10**, 21–33.
13 M. Cohen, D. Joester, I. Sabanay, L. Addadi, B. Geiger. *Soft Matter.* 2007, **3**, 327–332.
14 S.P. Evanko, M.I. Tammi, R.H. Tammi, T.N. Wight. *Adv. Drug Deliv. Rev.* 2007, **59**, 1351–1365.
15 J.P. Xiong, T. Stehle, R.G. Zhang, A. Joachimiak, M. Frech, S.L. Goodman, M.A. Arnaout. *Science* 2002, **296**, 151–155.
16 M.D. Pierschbacher, E. Ruoslahti. *Nature* 1984, **308**, 30–33.
17 U. Hersel, C. Dahmen, H. Kessler. *Biomaterials* 2003, **24**, 4385–4415.
18 Y. Lai, C. Xie, Z. Zhang, W. Lu, J. Ding. *Biomaterials* 2010, 31, 4809–4817.
19 M. Cohen, D. Joester, B. Geiger, L. Addadi. *Chem. Bio. Chem.* 2004, **5**, 1393–1399.
20 J.M. Curran, R. Chen, JA. Hunt. *Biomaterials* 2010, **31**, 1463–1464.
21 D. Trimbach, B. Keller, R. Bhat, S. Zankovych, R. Pohlmann, S. Schroter, J. Bosert, K. D. Jandt. *Adv. Funct. Mater.* 2008, **18**, 1723–1731.
22 M. Cicuéndez, M.T. Portolés, I. Izquierdo-Barba, M. Vallet-Regí. *Chem. Mater.* 2012, **24**, 1100–1106.
23 A. Butscher, M. Bohner, S. Hofmann, L. Gauckler, R. Muller. *Acta Biomaterialia* 2011, 7, 907–920.
24 A. García, I. Izquierdo-Barba, M. Colilla, C. López de Laorden, M. Vallet-Regí. *Acta Biomaterialia* 2011, **7**, 1265–1273.
25 H.S. Yun, S.E. Kim, Y.T. Hyeon. *Chem. Comm.* 2007, 2139–2141.
26 M. Malmsten. *J. Colloid Interface Sci.*1994**, 166**, 333–342
27 M. Cicuéndez, I. Izquierdo-Barba, S. Sánchez-Salcedo, M. Vila, M. Vallet-Regí. *Acta Biomaterialia* 2012, **8**, 802–810.
28 A.H. Reddi, C.B. Huggins. *Proc. Soc. Exp. Biol. Med.* 1972, **140**, 807–810.
29 S.J. Hollister. *Nat. Mater.* 2005, **4**, 518–524.
30 J.R. Jones, L.M. Ehrenfried, L.L. Hench. *Biomaterials* 2006, **27**, 964–973.
31 I. Medved, R. Cerny. *Micro Mesoporous Mater*. 2011, **142**, 405–422.
32 S. Padilla, I. Izquierdo-Barba, M. Vallet-Regí. *Chem. Mater.* 2008, **20**, 5942–5944.
33 M. Vallet-Regí. *J. Intern. Med.* 2010, **267**, 22–43.
34 M. Vallet-Regi. *ISRN Mater. Sci.* 2012, Article ID 608548, 20 pages.
35 M. Cicuéndez, I. Izquierdo-Barba, M. Portolés, M. Vallet-Regí. *Eur. J. Pharm. Biopharm.* 2013, **84**, 115–124.
36 T.J. Webster, C. Ergun, R.H. Doremus, R.W. Siegel, R. Bizios. *J. Biomed. Mater. Res. A* 2000, **51**, 475–483.
37 S.F. Lamolle, M. Monjo, M. Rubert, H.J. Haugen, S.P. Lyngstadaas, J.E. Ellingsen. *Biomaterials* 2009, **30**, 736–742.
38 R.Z. Legeros. *Clin. Orthop. Relat. Res.* 2002 **395**, 81–98.
39 F. Zhang, M.P. Srinivasan. *Langmuir* 2004, **20**, 2309–2314.
40 M. Colilla, I. Izquierdo-Barba, S. Sanchez-Salcedo, J.L.G. Fierro, J.L. Hueso, M. Vallet-Regi. *Chem. Mater.* 2010, **22**, 6459–6466.
41 M.P.J. Peeters, W.J.J. Wakelkamp and A.P.M. Kentgens. *J. Non-Cryst. Solids* 1995, **189**,77–84.
42 P. Innocenzi, Y.L. Zub and V.G. Kessler, Sol-Gel methods for materials processing, Springer Science, Netherlands, 2008.
43 S. Sánchez-Salcedo, M. Colilla, I. Izquierdo-Barba and M. Vallet-Regí. *J. Mater. Chem. B* 2013, **1**, 1595-1606.
44 L.G. Griffith, G. Naughton. *Science* 2002, **295**, 1009–14.
45 N.G. Maroudas. *J. Theoretical. Bio*. 1975, **49**, 417-24.
46 H.A. Scheraga, J.R. Laskowski, Adv. Prot. Chem. 1957, **12**, 2–5.
47 B. Lassen, M. Malmsten. *J. Colloid. Interface. Sci.* 1997, **186**, 9–16

Prof. María Vallet-Regí,
Departamento de Química Inorgánica y Bioinorgánica
Facultad de Farmacia
Universidad Complutense
28040, Madrid, Spain
Tels: +34-913941861/3941843; FAX: +34-91-3941786
e-mail: vallet@farm.ucm.es

Madrid, October 17th 2013

Dear Dr Stephen Hessey,

Thank you very much for your kind e-mail concerning the Manuscript **ID: TB-ART-09-2013-021307**, entitled **"Tailoring hierarchical meso-macroporous 3D scaffolds: From nano to macro"** authored by *Mónica Cicuéndez, Martin Malmsten, Juan Carlos Doadrio, María Teresa Portolés, Isabel Izquierdo-Barba and María Vallet-Regí.*

We sincerely appreciate reviewers' remarks to improve the article and we have modified our manuscript following their recommendations. The modifications are highlighted in the manuscript and detailed responses to the reviewers' comments are included bellow.

We hope that the revised version of our manuscript is now appropriate for publication in Journal of Materials Chemistry B.

Thank you for your kind consideration of our work.

Sincerely,

Prof. María Vallet-Regí.

Response to the Reviewers:

Reviewer #1

Comments to the Author:

Using simple chemistry, the authors have successfully modified the surface of mesoporous glass – hydroxyapatite nanocomposite scaffold with amine groups. The manuscript is very well presented and the experimental design is perfect.

The authors thank very much all referee comments.

Major Comments:

There are no major comments; however, the mechanical behavior of such scaffolds is not addressed.

Certainly, the authors totally agree with the referee´s comment when he/she falls upon on the mechanical properties of scaffolds. In this sense, these properties are one of the main factors of 3D scaffolds to taken into account for bone tissue regeneration applications. So far, the resulting MGHA scaffolds obtained by rapid prototyped and subsequently calcination exhibits a good handling, not being necessary any specific coating with polymers, as it happens with scaffolds based on foams. This fact is a highly important feature when they are used both *in vitro* in cellular assays and *in vivo* assays. Thus, a deep study concerning the mechanical properties of these MGHA scaffolds in collaboration with other research group is being carried out to determine in different parameters such as compressive strength, hardness, young's modulus, among others. Moreover, a monitorization of these properties as function of *in vitro* scaffold degradability in presence of several cell types is also performed. The results will be the aim of another more specific future manuscript.

Minor comments:

- The reviewer wonder: Is there any effect of the amine surface functionalization on the bioactivity and ionic release of the modified scaffold?

The authors appreciate the referee´s comment; *In vitro* bioactivity after functionalization process has been checked, showing any difference with respect to unmodified material. MGHA-NH_2 material exhibits high bioactivity process with similar kinetic that unmodified ones. Concerning the ionic variation of calcium, phosphorous and silicon in SBF after soaking the MGHA-NH_2 material, the ICP measurements showed any difference in the first times of incubation with respect to unmodified material. This similar behavior is probably due to that the amine functionalization process does not affect to both the glass mesoporous arrangement (textural properties and silica connectivity) and apatite nanocrystalline component of the MGHA *nanocomposite,* as it has been described on the manuscript. In this sense, the *in vitro* bioactive behavior after amine modification have not included because this manuscript has been addressed mainly to study the role of these amine moieties on the osteoblast behavior (cell attachment, proliferation, differentiation, etc.) as well as the mechanisms that govern this interaction by ellipsometry study.

- Section 2.1.: Please, correct the typographical error in line #5.

The authors thank the referee´s comment and the typographical error in line #5 of the section 2.1. has been corrected.

- Section 2.3. : Please, mention the degassing conditions (temperature and time) used prior to the BET analysis of MGHA and MGHA-NH2 scaffolds.

The authors appreciate the referee´s comment and a new paragraph detailing the degassing conditions for N_2 adsorption measurements has been incorporated in the section 2.3. of the manuscript, as follows:

"Prior to these measurements, both MGHA and MGHA-NH_2 scaffolds were degassed at 60ºC during 24 hours under vacuum (<0.3 kPa)."

Referee #2

Comments to the Author:

This work develops novel meso-macroporous 3D scaffolds for bone tissue regeneration. The results show that the amine chemical modification of scaffold's surface significantly improves the potential of these materials for bone tissue regeneration applications. Overall a good article with a few things needs to be changed. The abstract and the conclusion sections look like same. There are similar sentences in these sections. These sections should be re-written.

The authors thank very much the referee´s comments and they totally agree with her/his appreciation. Thus, the authors have re-written the abstract and conclusion sections, removing the similar sentences in these sections, as follow:

Abstract

"Bone tissue regeneration requires the use of 3D scaffolds which mimic the architecture of the natural extracellular matrix, creating an adequate microenvironment for bone cell growth. Such 3D scaffolds need surface properties suitable to biological recognition in the early stage of cell adhesion, necessary to assure complete cell colonization, retained cell functionality, and subsequently bone regeneration. Herein, hierarchical 3D scaffolds based on new hydroxyapatite/mesoporous glass nanocomposite bioceramic (MGHA) exhibiting different scales of porosity have been synthesized. These possess: (i) highly ordered mesopores with diameters of 10 nm; (ii) macropores with diameters in the 30–80 μm range with interconnections of 1-10 μm; and (iii) large macropores of ca. 500 μm. To improve their surface properties, 3D scaffolds were modified through direct functionalization with amine propyl groups, which notably improves preosteoblast

adhesion, proliferation (2.3 fold), differentiation (4.8 fold) and further cell colonization of these scaffolds. The observed enhancement can be related to these amine groups which favour early adhesion, e.g., based on nonspecific protein adsorption as was demonstrated by ellipsometry. These results suggest that the combination of hierarchical structure design and amine surface modification of hydroxypatite/mesoporous nanocomposite scaffolds, yields a double increase in cell proliferation, as well as quadruple increase in cell differentiation, demonstrating the potential of these nanocomposite materials for bone tissue regeneration purposes."

Conclusions

"*3D scaffolds based in a new nanocomposite (MGHA) composed by hydroxyapatite nanocrystalline embedded into mesoporous glass have been fabricated through rapid prototyping technique. The 3D MGHA scaffolds exhibit three scales of porosity: ordered mesopores (10nm), interconnected macropores (1-80μm), and ultra-large macropores (500μm). This hierarchical meso-macroporous system is obtained by using a sol precursor containing different scale-length polymers (Pluronic F127 and methylcellulose as meso and macrostructure directing agents, respectively) together with a robocasting process. The surface properties of these MGHA scaffolds, concerning cell recognition have been enhanced through a direct functionalization with aminopropyl moieties. This simple and cost-effective amine modification causes noticeable improvements in the preosteoblast adhesion, as well as a double increase in cell proliferation and a quadruple increase in cell differentiation. Moreover, ellipsometry studies demonstrated that the protonated amino propyl moieties favour the early step in the adhesion process by an increase in the nonspecific protein adsorption. Therefore, these studies reveal that both the structure design of hierarchical meso-macroporous 3D MGHA scaffolds and the amine chemical modification of their surface significantly improve the biocompatibility of these nanocomposite scaffols*".